Title

Resolving Ambient Organic Aerosol Formation and Aging Pathways with Simultaneous Molecular Composition and Volatility Observations

Journal

ACS Earth and Space Chemistry, 4(3)

ISSN

2472-3452

Authors

Lee, Ben H
D'Ambro, Emma L
Lopez-Hilfiker, Felipe D
et al.

Publication Date

2020-03-19

DOI

10.1021/acsearthspacechem.9b00302

Peer reviewed

Published in final edited form as:
ACS Earth Space Chem. 2020 March 19; 4(3): 391–402. doi:10.1021/acsearthspacechem.9b00302.

Resolving ambient organic aerosol formation and aging pathways with simultaneous molecular composition and volatility observations

Ben H. Lee[1,†], **Emma L. D'Ambro**[2,†,‡], **Felipe D. Lopez-Hilfiker**[1,§], **Siegfried Schobesberger**[1,‖], **Claudia Mohr**[1,¶], **Maria A. Zawadowicz**[3], **Jiumeng Liu**[3,#], **John E. Shilling**[3], **Weiwei Hu**[4,††], **Brett B. Palm**[4,‡‡], **Jose L. Jimenez**[4], **Liqing Hao**[5], **Annele Virtanen**[5], **Haofei Zhang**[6,§§], **Allen H. Goldstein**[6], **Havala O. T. Pye**[7], **Joel A. Thornton**[1,*]

[1]Department of Atmospheric Sciences, University of Washington, Seattle, WA, U.S.A. [2]Department of Chemistry, University of Washington, Seattle, WA, U.S.A. [3]Atmospheric Sciences and Global Change Division, Pacific Northwest National Laboratory, Richland, WA, U.S.A. [4]Cooperative Institute for Research in Environmental Sciences and Department of Chemistry, University of Colorado, Boulder, CO, U.S.A. [5]Department of Applied Physics, University of Eastern Finland, Kuopio, Finland. [6]Department of Environmental Science, Policy, and Management, University of California, Berkeley, CA, U.S.A. [7]Office of Research and Development, Environmental Protection Agency, Research Triangle, NC, U.S.A.

Abstract

Organic aerosol (OA) constitutes a significant fraction of atmospheric fine particle mass. However, the precursors and chemical processes responsible for a majority of OA are rarely conclusively identified. We use online observations of hundreds of simultaneously measured molecular components obtained from 15 laboratory OA formation experiments with constraints on their effective saturation vapor concentrations to attribute the VOC precursors and subsequent chemical pathways giving rise to the vast majority of OA mass measured in two forested regions. We find that precursors and chemical pathways regulating OA composition and volatility are dynamic over

*Corresponding author: Joel A. Thornton (joelt@uw.edu).
†Equally contributing co-authors
‡Now at the Oak Ridge Institute for Science and Education, US Environmental Protection Agency, Research Triangle Park, NC, USA.
§Now at TofWerk AG, Thun, Switzerland.
‖Now at University of Eastern Finland, Kuopio, Finland.
¶Now at Stockholm University, Stockholm, Sweden.
#Now at Harbin Institute of Technology, Harbin, China.
††Now at Guangzhou Institute of Geochemistry, Chinese Academy of Sciences, Guangzhou, China.
‡‡Now at University of Washington, Seattle, WA, U.S.A.
§§Now at University of California, Riverside, CA, U.S.A.

Author Contributions

The manuscript was written through contributions of all authors. All authors have given approval to the final version of the manuscript. †These authors (Ben H. Lee[1,†], Emma L. D'Ambro[2,†]) contributed equally.

Supporting Information.

Supplemental Figures S1–S11 and tables S1 and S2 (PDF).

The US Environmental Protection Agency through its Office of Research and Development collaborated in the research described here. The research has been subjected to Agency administrative review and approved for publication. The views expressed in this article are those of the authors and do not necessarily represent the views or policies of the U.S. Environmental Protection Agency.

hours to days, with their variations driven by coupled interactions between multiple oxidants. The extent of physical and photochemical aging, and its modulation by NO_x, were key to a uniquely comprehensive combined composition-volatility description of OA. Our findings thus provide some of the most complete mechanistic-level guidance to the development of OA descriptions in air quality and Earth system models.

Graphical Abstract

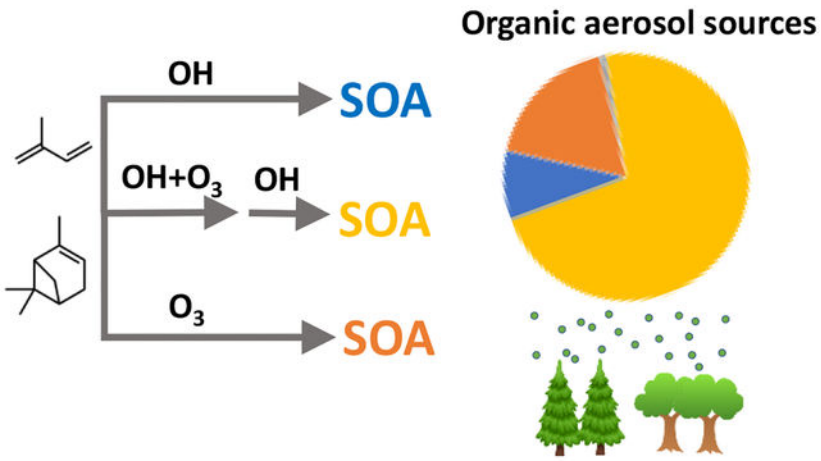

Keywords

source and chemistry attribution; atmospheric simulation chamber; ambient measurements

Introduction

Atmospheric fine aerosol particles affect climate through alteration of Earth's energy balance[1] and are a major contributor to degraded air quality with strong links to premature mortality and other adverse health effects[2]. Identifying the chemical and physical processes which regulate fine particulate mass is thus of great interest for air quality policy, public health assessments, and studies of climate sensitivity. Organic carbonaceous material is a major and often dominant component of ambient fine particle mass[3], known as organic aerosol (OA). On regional and global scales, most OA is of secondary origin[4], being formed in the atmosphere via *in situ* chemical reactions that lead to gas-to-particle conversion of reactive organic vapors. Atmospheric oxidants, such as ozone (O_3), hydroxyl radical (OH), and nitrate radical (NO_3) react with a suite of organic vapors to form an even more complex and diverse array of products, a fraction of which partition to, and/or react in, the particle phase forming secondary organic aerosol (SOA)[5].

Over continents, the main precursors to SOA in the regional background are biogenic volatile organic compounds (VOC)[6] such as isoprene, monoterpenes, and sesquiterpenes. In and downwind of urban areas, SOA is typically enhanced, indicating a role for anthropogenic VOC and potentially also a relative enhancement in the conversion of biogenic VOC into SOA by other anthropogenic emissions including nitrogen oxides, sulfur

dioxide, oxidants, and primary organic aerosol[7–10]. While the ubiquitous nature of OA and its major contribution to fine particle mass are now well recognized, typically a majority of SOA mass remains unattributed to specific precursors, and even less so to specific chemical and physical aging pathways. This limitation in turn prevents making accurate predictions about how SOA will change in response to anthropogenic emissions, as well as to land use and climate change.

Apportionment of ambient aerosol particle mass to specific sources by using a linear sum of the chemical products of known source profiles, i.e. chemical source apportionment, is well established[11]. Implementation of more efficient multi-linear regression techniques and utilization of evolving instrument capabilities continue to improve description of bulk properties as well as source attribution. Fundamentally, attribution not just to precursor or emission type, but to atmospheric chemical and physical processes of the precursors and OA itself is needed to improve descriptions of OA formation and evolution in air quality and Earth system models. Recent developments in analytical methods now allow routine probing of large fractions of OA mass at a molecular or elemental formula level on hourly or faster timescales[12–15]. The richness of molecular-level information in turn provides an opportunity for more robust attribution to chemical and physical processes.

We conducted a uniquely broad suite of field and atmospheric simulation chamber studies of time-resolved chemical formula-level SOA composition using the Filter Inlet for Gases and AEROsols (FIGAERO) coupled to an iodide adduct ionization high-resolution time of flight mass spectrometer (HRToF-CIMS), referred to as the FIGAERO-CIMS herein[12]. Distinct quantitative distributions of unique molecular composition ($C_xH_yO_zN_{0–1}$) observed in 15 laboratory chamber studies that employed a range of biogenic and anthropogenic VOC and chemical conditions are used as the basis to explain hourly OA molecular spectra observed with the same instrument at two field measurement sites: a temperate forest location as part of the Southern Oxidant and Aerosol Study (SOAS) in Centreville, AL in June-July of 2013[16], and a boreal forest location as part of the Biogenic Aerosols–Effects on Clouds and Climate (BAECC) experiment in Hyytiälä, Finland in April-May of 2014[17].

The range of precursors and chemical processing regimes probed in the laboratory represent both remote and polluted environments, and atmospheric aging timescales from hours to several days. These studies allow us to account for >90% of the variance in the mass concentration distributions of 175 and 203 specific molecular compositions at SOAS and BAECC, respectively, that in turn explain 77% to 88% of the total OA mass as observed in each location by a high resolution time-of-flight aerosol mass spectrometer[18] (Figures S1 and S2). We are therefore able to provide comprehensive new constraints not only on the dominant precursor combinations but also on the chemical conditions and aging pathways that are consistent with the simultaneous molecular composition and volatility of ambient OA. These results are a key test to air quality models that incorporate SOA formation, especially from biogenic hydrocarbons, as a function of oxidation pathway, as well as a roadmap for future atmospheric simulation chamber studies to target specific VOC-chemical condition pairings that are relevant to the ambient atmosphere.

Methods

Instrument package

The Filter Inlet for Gases and AEROsols was coupled to a high-resolution time-of-flight chemical ionization mass spectrometer (FIGAERO-CIMS) utilizing iodide-adduct ionization for the measurements presented herein[12, 19]. Atmospheric simulation chamber experiments were conducted at the Pacific Northwest National Laboratory (Richland, WA) in a 10.6 m^3 FEP chamber[20]. The identical instrument package was housed in a trailer located in a clearing in the field in Centreville, AL (33.18 °N, 86.78 °W) during SOAS and at the top of a 35 m tall scaffolding tower in Hyytiälä, Finland (61.50 °N, 24.17 °E) during BAECC. Suspended particles in the ambient atmosphere or laboratory chamber were collected onto a 2.0 μm pore size PTFE filter (Pall Corp.) while the gas-phase was measured. A custom inertial impactor was used to remove particles > ~2 μm prior to collection of ambient particles. Two separate inlets were utilized for gas and particle phase sampling: PTFE for gas-phase and stainless steel for particle-phase measurements. The duration of particle collection/gas-phase measurements was between 10 and 40 minutes, depending on aerosol loading. Collected particles were desorbed from the filter and subsequently measured by the CIMS by gradually heating constantly flowing (2.0 slpm) UHP N_2 at a rate of 10°C min^{-1} from room temperature up to 200°C and held for 25 to 45 minutes depending on loading, then cooled back to room temperature over a 10 minute period, at the end of which the signal for most compounds typically returned to levels before the start of desorption. Instrument background of particle-phase measurements was determined by programmatically inserting a secondary 2.0 μm pore size PTFE filter upstream of the main filter before the start of every fourth collection cycle to account for any low-volatile gaseous compounds that may adsorb onto the filter and other artifacts that may arise during heating.

Basis set compilation and apportionment

We utilize 15 laboratory chamber experiments probing the formation and evolution of SOA from multiple precursors: (10) monoterpene, (2) isoprene, (1) isoprene epoxydiol, (1) sesquiterpene, and a (1) fossil fuel derived vapor, trimethyl benzene. More than 50 chamber experiments in continuous mode and 19 in batch mode were conducted at PNNL, focusing mainly on monoterpenes or isoprene. All but 15 OA mass spectra were rejected for this source apportionment work because the rest were not sufficiently different from these 15, in terms of conditions probed (Figures S3 and S4), hence, the composition of the resulting SOA. Out of the 10 monoterpene experiments included in the basis set only a few contributed significantly to the composite, as shown in Table S1, but were kept in the basis set to demonstrate which chemical conditions − for instance, the level of NO_x and the extent of photochemical aging − yielded the OA compositions that matched those of the field and which did not. As such, the goal here was not to determine the minimum number of basis set members needed, but to identify the chemical conditions needed to yield the mass spectra that, together, best resembled that of ambient OA.

A composite spectrum was constructued to match each of the ~hourly submicron OA molecular composition spectrum observed in the ambient atmosphere during SOAS and BAECC. The composite spectra are optimal combinations (x) of our molecular composition

basis sets (C), determined to minimize the residual with the ambient OA molecular composition spectra (d), as described by eq. 1.

$$\min_{x} \|C \cdot x - d\|_2^2, \; where \; x \geq 0 \qquad \text{(eq. 1)}$$

The starting basis set is comprised of 15 distinct OA mass spectra obtained in laboratory chamber experiments with varying VOC precursors and chemical conditions (Figures S3 and S4). The OA composition was determined by integrating the sum of the signals of each organic compound ($C_xH_yN_{0,1}O_z$) detected during each full desorption cycle, that is, the signal dependence on desorption temperature is not considered for the apportionment. Following apportionment, the volatilities of ambient OA and the composite are compared, as shown below.

All ten of the monoterpene and both isoprene OA mass spectra included in the basis set were obtained from experiments conducted in continuous mode −that is, the OA mass spectra changed little after steady state was obtained − of varying photochemical ages. Because these experiments were conducted in steady state mode, the SOA compositions are an integration of organic material that had undergone a range of photochemical processing. As such, the OH-equivalent ages of OA reported below encapsulate the extent that α-pinene is oxidized solely by OH, but do not account for chemistry involving other oxidants, oxidation of later-generation products, or multi-phase chemistry. Each of the ~hourly OA mass spectra measured during the course of all 19 batch mode experiments (which lasted anywhere from 14 to 49 hours and during which the OA composition evolved, as shown for two of those experiments in Figures S5 and S6) were also tested to determine their similarity against the field OA mass spectra from both sites. None contributed significantly to the field-matched composites.

The 15 basis spectra derived from controlled laboratory experiments alone explain 75% and 77% of the variance in the atmospheric OA molecular spectra over the durations of SOAS and BAECC, respectively. Additional spectra (five for SOAS and two for BAECC), distinct from one another and from the 15-member basis set, were identified as residual spectra − or the difference between the composite and the ambient OA − to include as part of the basis set. The residual spectra were iteratively added to the basis set in order of descending total OA mass each represented until the increase in the agreement between the aggregate of all of the hourly ambient OA spectra and composites from each field campaign were negligible and/or the OA mass of the composite exceeded that of the ambient. As such, the five residual spectra included in the basis set for SOAS and two for BAECC illustrate OA mass that was consistently present in the ambient that was missing from our laboratory experiments (Figures S7 and S8). Three of the residuals from SOAS and one from BAECC had characteristics of biomass burning organic aerosol (BBOA) (Figure S7), composed primarily of $C_6H_{10}O_5$ (presumably levoglucosan, a byproduct of biomass combustion[21]) and explained an additional 4% and 2% of the OA mass on average, respectively. The remaining “other” residual spectra − two for SOAS and one for BAECC − were pronounced during daytime, dominated by C_4-C_6 compounds, and explained an additional 10% and 5% of OA mass at SOAS and BAECC, as shown below. We included these residual representative

spectra in the final basis set. Additional residual spectra did not improve the overall attribution or mass closure.

We also examined SOA formation and evolution from three monoterpenes: α-pinene, Δ−3 carene, and β-pinene. Limonene, which has two C=C double bonds, was not tested under comparable conditions. Given that the FIGAERO-CIMS only resolves molecular composition, and not structural isomers, we expected that SOA from these monoterpenes would appear similar. While this expectation was largely met, spectra were not identical (Figure S9). That said, without further structural information, we do not attempt to speciate SOA precursors beyond the general monoterpene category as a result of the broad similarities in molecular composition produced by their oxidation. The 10 monoterpene oxidation experiments included in the basis set are from α-pinene, which was tested most extensively under varying chemical conditions during these experiments at PNNL. The extent of oxidation ranged from a few hours to several days of equivalent photochemical aging in the atmosphere (assuming 1×10^6 OH molecules cm^{-3} over an 8-hour day), across actual chamber residence times from 3 to 12 hours. The experiments in which the photochemical aging was >3.5 days and wherein the fraction of monoterpenes reacting with OH was ~0.6 yielded OA mass spectra that agreed the best with those of the field, as discussed below. Only α-pinene was tested under such conditions. Dark oxidation in the presence of NO_3 and O_3, likewise, was only extensively tested for α-pinene.

Monte Carlo approach

In addition to the above least-squares approach, we utilized a randomized Monte Carlo approach to the selection and weighting of basis set members, and found largely comparable. Ten thousand simulations − in which a randomized set of weights was assigned to each of the input basis spectrum, all together summing up to one − was performed for each of the hourly field-observed OA composition measurements. The Monte Carlo approach yielded similar but slightly inferior fits (R^2=0.86) to those of the non-negative linear least-squares approach (R^2=0.93), as shown in Figure S10. The reason for its subpar performance was that by requiring the sum of the weights to be a constant value (one), the distribution in the weights of a given spectrum was no longer random. Increasing the number of simulations did not consistently improve the performance of the fits. In addition to confirming the broad results of the least squares attribution, the Monte Carlo approach also demonstrates that the subtle differences in the basis set OA spectra, and hence, the chemical conditions that produced them, are distinguishable given that the slightly different distribution of weights among basis set members achieved with the Monte Carlo approach leads to a different, sub-optimal, agreement between the composite and ambient spectra (Figure S10).

CMAQ v5.3

Community Multiscale Air Quality (CMAQ) Model (version 5.3) was used to simulate total OA loading from 1 June to 15 July (overlapping with SOAS season) and 15 April to 31 May (overlapping with BAECC season) conditions at 108×108 km horizontal resolution, both for the year 2016. The sources of OA are listed in Table S2. The SOAS and BAECC campaigns were conducted in the years 2013 and 2014, respectively. Thus, the main point of

comparison between the model and analysis presented here is of the composition of OA, as presented in Figure 2. Details of these simulations, including the treatment of primary organic aerosol[22], SOA from monoterpene oxidation by OH and ozone[23], explicit hydrolysis of organic nitrates[24], acid-catalyzed isoprene epoxide reactions[25], semi-volatile isoprene and sesquiterpene oxidation products[26], glyoxal uptake on aerosols[27] and cloud droplets[28], as well as the oxidation of traditional anthropogenic VOCs are provided elsewhere[26–27] (http://www.github.com/USEPA/CMAQ; doi: 10.5281/zenodo.3379043).

Results and Discussion

Ambient OA source apportionment

Using optimal combinations of the OA molecular composition basis set, we can explain on average 90% and 92% of the observed variance in OA molecular composition observed during SOAS and BAECC, respectively, as shown in Figure 1. The resulting basis set composites also explain greater than 75% of the total OA mass (Figure S1). Thus, while the basis set derived from laboratory experiments does not account for all possible VOC precursors and processing pathways, that the composites explain a large fraction of the OA mass and variance in the field-observed molecular spectra suggests such unaccounted for precursors or pathways are likely not dominant drivers of the total OA mass at these two sites. Details on the basis set and OA composite determination are provided in Methods.

As illustrated in Figure 2 (a and b), the contribution of different basis set members to the median composites reveal key insights into not only the dominant VOC precursors, but also the chemical and physical processing driving the formation and evolution of OA in each location. The latter information has generally been lacking from OA source apportionment, and the combination of both precursor and evolution pathway constraints illustrates gaps in our description of OA in state-of-the-art air quality models (Figures 2c and 2d). We find that on average, the photochemical oxidation of monoterpenes in the presence of both O_3 and OH simultaneously, accounted for the largest fraction of OA in both locations, thus highlighting the importance of synergistic oxidation[29] of VOC for describing ambient OA. Differences between the two locations in terms of overall apportionment were found in the relative importance of dark ozonolysis of MT, with and without NO_3, as well as in the role of isoprene multiphase chemistry, biomass burning, and other unidentified precursors or pathways. Overall, oxidation of monoterpenes contributed on median 65% during the SOAS campaign, consistent with the findings of *Zhang et al.*[30], and 86% of OA mass during the BAECC campaign.

The Community Multiscale Air Quality (CMAQ) Model is used to evaluate responses of air quality of past and future policy changes. Here, we find that the model broadly captures the importance of monoterpenes in the temperate Alabama forest location while significantly underpredicting their importance in the boreal forest location in place of a larger role for primary organic aerosol (POA) and SOA derived from anthropogenic VOC. Moreover, the relative importance of sesquiterpenes, glyoxal, and the oxidant drivers such as ozone and OH are rather different in the model predictions compared to our attribution. That such differences exist is not surprising, but highlights how the combined precursor-evolution

pathway information can provide strong tests to model descriptions and inform new directions for model development.

The distribution of organic mass as a function of carbon atom number groups (nC) observed at SOAS and BAECC (Figure 3a) provides a simpler composition view of the underlying apportionment. We find that the nC distributions observed in ambient OA are best reproduced by the laboratory experiments oxidizing α-pinene (Figure 3b). The nC distributions of chamber-generated SOA derived from IEPOX, β-caryophyllene, and TMB (Figure 3c) were shifted to higher or lower nC than the bulk of OA observed in the field locations (Figure 3a). Thus, our apportionment technique clearly rules out a substantial contribution from sesquiterpenes as represented by β-caryophyllene and aromatics represented by 1,2,4-trimethylbenzene (TMB) in these two locations.

In general agreement in the CMAQ predictions, our analysis suggests limited importance for isoprene contributions to OA via both low and high NO_x photochemical oxidation, as well as by acid catalyzed multiphase chemistry of IEPOX, which we find to be less than 25% of the median OA measured at the Southeast United States (SEUS) site during summer, consistent with prior estimates made using different methods[30–34]. Isoprene derived SOA made an even lower contribution (~5%) at the Finnish boreal forest site during the spring-summer transition as expected given the timing of deciduous tree leaf-out and the light and temperature dependence of isoprene emissions. The SOAS campaign took place in a region populated mostly by isoprene-emitting broadleaf trees, while BAECC took place at a boreal forest dominated by fir and spruce, during the spring leaf-out transition with temperatures significantly lower than at SOAS. That isoprene photochemical SOA components were negligibly detected at the BAECC location where isoprene emissions are low is thus consistent with the different mix of vegetation across the typical fetches of the two locations, and an example of the lack of false-positives of this apportionment method.

Diurnal variability in OA composition

A composite of basis set members is produced for each approximately hourly determination of OA molecular composition. Locally dynamic sources of SOA and the importance of multi-day aging are evident in the diurnal patterns of the relative importance of specific basis spectra shown in Figure 4, and provide additional important context to the summary attribution in Figure 2. Our observations of OA composition are sensitive to total mass, and are made at a fixed location. As SOA mass integrates over the lifetime of an aerosol particle, the local addition (or loss) of SOA mass at our receptor sites becomes a smaller fraction of the components we observe. Consistent with this perspective, the ambient OA attributed to the two experiments with the most photochemical aging of α-pinene SOA showed negligible diurnal variability (Figures 4a and 4b). The lack of diurnal variations in the relative contribution of these pathways suggests the composition and properties of this SOA reflect that of the regional background, consistent with these experiments producing SOA with the lowest effective volatility and equivalent photochemical ages of 3 to 5 days.

Contributions from other pathways and VOC precursors had notable diel cycles implying more dynamic OA components as shown in Figure 4, though we note that the y-axis scale changes for each component to illustrate the variation. The basis spectra representing SOA

from isoprene oxidation reached peak contributions during the daytime in the SOAS campaign, consistent with those reported previously[32–37], and with its daytime emission. A diurnal maximum in the daytime suggests that isoprene photochemical SOA is produced locally, albeit at low levels, but has a short lifetime (~1 day) that limits its accumulation relative to other sources into the regional background. Notably, the OA contribution from IEPOX reactive uptake has a less pronounced decrease from its midday maximum, consistent with the majority being low volatility[32, 34, 38] and unreactive. In the Finnish boreal forest site, isoprene derived SOA was nearly negligible as noted above, especially in a local context.

The basis spectra representing molecular components from NO_3-initiated oxidation of monoterpenes in the presence of O_3 exhibited a characteristic diurnal trend at both sites peaking in contribution at night and reaching a minimum during late afternoon (Figures 4e and 4f). Such a diurnal trend suggests NO_3 driven monoterpene SOA is produced locally at both sites, but also that a significant loss of the initially-formed products limits its accumulation into the regional background SOA, as suggested by the higher volatility of SOA formed from the dark oxidation of α-pinene in the presence of O_3 and NO_3 (Figure S4). The amount of OA mass contributed by NO_3-initiated chemistry was much less during the SOAS campaign compared to BAECC campaign (2% vs 35%, nighttime maximum), even though the nighttime NO_x loading was typically higher during SOAS, suggesting either a more efficient production of particulate organic nitrates (pON) during the BAECC campaign, or a faster loss rate of pON at SOAS[20, 24, 39–42]. For instance, very rapid hydrolysis of pON was recently postulated by *Zare et al*.[43]. We cannot conclusively rule out ON hydrolysis based on the field spectra alone. Recently, *Takeguchi et al*.[44] showed that less than 35% of nitrates formed from monoterpene oxidation undergo hydrolysis, and that hydrolysis may not be the dominant fate of the respective pON, consistent with our recent experiments (Figure S5). We observed more significant loss of pON formed under dark conditions during subsequent photochemical aging at moderate humidity (50% RH) (Figure S5), consistent with the work of *Nah et al*.[45].

The multiphase chemistry of pON presents a potential challenge to attributing a direct role for NO_x, typically parameterized in models using "high NO_x" or "low NO_x" SOA yields from chamber experiments based on the model calculated fraction of RO_2 reacting with NO compared other RO_2 fates. As we infer a large fraction of OA at both sites is days old, the fate of local RO_2 is not illustrative of the actual role of NO_x on the majority of OA mass measured at these locations.

Evolution of OA composition and volatility and the role of NO_x

The composition and volatility of SOA produced by α-pinene oxidation in laboratory experiments varied with photochemical age and the relative importance of OH and O_3 as oxidants (Figure S11). Specifically, overall volatility decreased with increasing photochemical age, consistent with the findings of *Donahue et al*.[46], as did the fraction of SOA molecular components with 10 carbon atoms (nC = 10) (Figure S11). The overall composition shifted to smaller nC components that desorbed at higher temperatures with

photochemical aging, consistent with thermal cracking of low volatility monomers and accretion products into daughter products upon thermal desorption[34, 47].

This dependence of both composition and volatility on aging timescale allows a further test of our attribution technique because the composite spectra were constructed by optimizing the agreement in OA molecular composition only, not volatility. We therefore compare the effective desorption temperature of a given component ($C_xH_yO_zN_{0–1}$) in the composite, to its counterpart measured in the ambient OA. The effective desorption temperature of a composite member is the average of that in all basis spectra weighted by their respective contributions to the composite. These effective desorption temperatures agreed well with the corresponding counterparts from the ambient OA spectra (Figure 5b). The sum of the desorption profiles of all compounds in the composite, similarly, agreed well with the summed desorption profiles observed during SOAS (Figure 5a). The agreement in both composition and volatility required experiments with photochemical aging of the SOA for an atmospheric equivalent duration of 3.6 to 4.5 days (assuming 8-hours of sustained OH levels of 1×10^6 molecules cm^{-3} equals one day of photo-chemical aging), and those in which the fraction of monoterpenes reacting with OH (f_{MT+OH}) was approximately 0.6 (experiments 4 and 9 in Figure S3 and Table S1), as illustrated in Figure S11. Experiment in which f_{MT+OH} was lower at ~0.45 and comparably aged to 4.6 days (experiment 10 in Figure S3) did not yield OA composition or volatility (Figure S11) that closely resembled those of the ambient. Experiments in which $f_{MT+OH} \geq 0.7$ (experiments 1–3 in Figures S3 and Table S1), likewise, did not significantly contribute to the composite. The OA formed in these experiments though were not as photochemically aged as those in which f_{MT+OH}~0.6, due in part to limits of generating sufficiently high OH levels without O_3 in steady state operation and chamber residence time. OA formed from α-pinene that was oxidized nearly solely by OH in batch mode allowed longer aging, albeit not at steady state. The composition of the OA formed was initially similar to that of experiment 1 (OH-age of 0.96 d), then approaches that of experiment 2 (OH-age of 1.6 d) and experiment 3 (OH-age of 2.3 d) as the OA ages, as shown in Figure S6. However, the OA compositions during this OH-dominant aging experiment do not ultimately have strong similarity to those of the ambient. These results demonstrate that the appropriate mix of oxidants as well as the extent of aging under those conditions are needed to reproduce the volatility and composition of OA observed in the field.

As noted, above, we found that to explain the OA composition and volatility observed in the field, the primary requirement was to produce SOA from α-pinene photo-oxidation at specific [OH] and [O_3]. As long as we controlled the steady state [OH] and [O_3], the composition and volatility of the SOA formed during photo-oxidation of monoterpenes with or without NO_x was largely similar (e.g., compare experiment 4 vs. 9 in Figure S4). This result is to be expected. First, pON were generally < 10% of the SOA mass even when [NO] ~ 0.6 ppb (Figure S3), consistent with a higher volatility of an -ONO_2 compared to an -OOH or ROOR group[48] and an alkyl nitrate yield from RO_2 + NO less than 0.5[49]. Thus, the most obvious direct effect of NO_x on photochemical SOA composition via N incorporation will be small on a mass weighted basis. Second, for [NO]<0.6 ppb, RO_2 autoxidation and the formation of low volatility non-nitrate HOM is likely to be largely unaffected given the fairly rapid unimolecular H-shift rates for 10–20% of primary RO_2[50–52]. That is, a major

SOA formation channel, via monoterpene-derived HOM[8, 53], was likely still operational in both the chamber experiments and the ambient atmosphere, thereby producing similar SOA composition and volatility even at significant NO_x concentrations. Third, our attribution approach does not allow insights into the SOA yield from the precursors and pathways, which may be affected by the presence of NO_x[54]. We note that for the range of [NO] probed in our experiments and expected to be impacting our field measurement locations, the effect of NO_x on monoterpene SOA yield is moderate after accounting for the NO_x impact on OH levels[55], consistent with our findings that controlled for the impact of NO_x on the chamber [OH] and [O_3]. Thus, our apportionment results suggest that the most important impact of NO_x on OA composition and volatility outside of urban regions is its indirect effect on the absolute and relative abundance of OH, O_3, and NO_3.

Our analysis explains a significant fraction of the variance in the chemical composition of OA, but it is not a complete description given the ~10 to 15% of unattributed mass (Figure S1) and the <10% accounted for by residuals which are not attributed to a specific precursor (Figures 4g and 4h). Processes or conditions not tested in our chamber experiments may help explain the remaining amount of unattributed OA, and/or may result in OA composition and volatility that is overall similar to our aging experiments. The basis spectra do not include a range of anthropogenic SOA precursors such as alkanes and most aromatics[56], photochemical processing in cloud water and aqueous particles[57], simultaneous oxidation of multiple VOCs[69,70], or effects of temperature[58]. Such features should be probed further.

Ding et al.[59] report using ^{14}C analysis at the SOAS site nine years prior to our measurements, and found that 21±4% of PM2.5 was comprised of carbon of fossil origin, while recent air quality modeling simulations predicted 2% (Figures 2c and 2d; Table S2) or 30% fossil contribution[60], highlighting the challenges associated with top-down OA source apportionment and trends in emissions. The unattributed fraction of OA mass from our apportionment, together with our measurement uncertainty, certainly allow for of order 10% contribution from fossil sources, but clearly constrain its contribution to be <20% of OA on average at these locations unless it is highly correlated with monoterpene SOA sources and has very similar composition and volatility, which we deem unlikely. Determining the origin of the unattributed OA mass in this work will potentially lend insight into other important ambient OA transformations.

Atmospheric Implications

Our results demonstrate that ambient SOA composition and volatility in biogenically influenced regions are dynamic over hours to days, and driven by coupled (simultaneous) interactions between multiple oxidants. The importance of sustained oxidation of a VOC precursor in the presence of multiple oxidants, as well as photochemical and physical aging, are clearly evident in our analysis of field spectra and consistent with insights from recent laboratory studies[29, 46]. Such interactions, between precursors, oxidants, and the aging extent, pose a challenge to adequately simulating SOA formation and evolution in chemical transport models and in laboratory chamber experiments. For example, beyond specific formation pathways, chemical and physical aging of SOA almost certainly involves specific mass loss pathways, such as photolysis[61–63] and evaporation[47, 64] leading to lower OA

volatility, and not just intrinsic changes to oxidation state. Such loss pathways will depend upon the initial formation mechanism, as well as particle phase transformations which affect SOA volatility[46].

Our comprehensive attribution approach supports the need to incorporate some of this complexity into models, given that simultaneous oxidation of monoterpenes and their products by OH, O_3, and NO_3 for 3 to 4 days of equivalent atmospheric aging were required to explain SOA composition and volatility in the two rural locations. Although the formation and evolution of SOA likely involves a complex interplay of multiple oxidants and timescales, the dominant precursors on regional scales at the two locations presented herein were well represented by a relatively simple set: α-pinene (monoterpenes), biomass burning, and isoprene, with the latter mostly via IEPOX multiphase chemistry. Our apportionment technique did not find significant contribution to ambient OA from anthropogenic precursors as represented by TMB, which is likely not an ideal proxy for such sources, but the contribution from other anthropogenic VOC precursors are still likely less than 20% of the OA in these regions given the fraction of submicron OA mass explained by our attribution.

NO_x has local direct effects on OA composition, via NO_3 oxidation and pON formation, but we infer a more indirect role given that we could explain a majority of ambient OA composition and volatility in these two locations using chamber experiments which produced monoterpene-derived SOA without added NO_x. The direct effect of NO_x, measured via the pON contribution to OA mass, in net was largest for the nighttime oxidation of monoterpenes by NO_3, on median 5% and 20% in the SEUS and Finnish locations, respectively, but with a significant diurnal cycle. As in the atmosphere, adding NO_x to the chamber experiments indirectly affects SOA by altering the relative and absolute amounts of OH, O_3, and NO_3 available to participate in the oxidation of VOC and subsequent OA processing. We conclude that if a direct role for RO_2 + NO is essential for understanding monoterpene-derived OA, it is likely through permutations of alkoxy radical products and the formation of HOM, perhaps by enhancing ring-opening in α-pinene derived RO_2 as suggested by *Kurten* et al.[65].

We observed very little ambient OA at either location consistent with that formed in a chamber after ~ 3 hours from OH oxidation of monoterpenes at low NO_x. Given the presence of monoterpenes and low-NOx conditions of both locations, this result may at first be surprising. That such “fresh” oxidation of monoterpenes explains a negligible fraction of the ambient SOA composition can be understood as being a result of the typical age of ambient particles and the variety of atmospheric oxidation pathways, of which SOA is an imperfect integrator. Atmospheric fine particles have residence times of a few days or longer, allowing for substantial chemical and physical modifications to, or losses of, SOA formed from one pathway. The diurnal cycles in the NO_3-driven pON components of OA are another example[41]. Thus, we conclude that SOA which forms promptly from OH oxidation of monoterpenes[8], is locally a small increment on top of the regional OA, and also evolves on timescales < 1 day *via* oligomerization, photochemical or heterogeneous loss pathways[66–68], or net evaporation[47, 64], so as to not accumulate above our measurement threshold (a few percent of OA).

Laboratory studies probing specific pathways (e.g. OH-only or NO_3-only) can provide mechanistic insights into specific reaction pathways, but our direct comparison to ambient OA composition and volatility suggests such experiments will likely not replicate biogenic SOA chemical or physical properties, which our analysis suggests are determined mostly by multi-oxidant interactions and associated aging. Thus, by extension, models employing pathway-specific SOA yields and/or lifetimes will also not likely represent SOA abundance and properties accurately without such synergies[29] and multi-phase aging timescales. Even purely physical aging of 24 hours or more can be essential to arrive at an SOA volatility representative of the ambient atmosphere[47], a timescale over which few chamber experiments are conducted but which is relatively short compared to the physical removal timescales of atmospheric aerosol. Our direct comparisons to ambient OA molecular composition and volatility bring these issues clearly into focus as likely needing attention for making progress on accurate descriptions of the SOA atmospheric life cycle.

Supplementary Material

Refer to Web version on PubMed Central for supplementary material.

ACKNOWLEDGMENT

BHL, ELD, FDL, SS, CM, and JAT were supported by a grant from the U.S. Department of Energy Atmospheric System Research Program (DE-SC0018221). ELD was supported by the National Science Foundation Graduate Research Fellowship (grant no. DGE-1256082). AV was supported by the Academy of Finland (grant No 317373, Center of Excellence programme grant No 307331) and the European research Council (ERC StG 335478). JES and JL were supported by the U.S. Department of Energy Office of Science, Office of Biological and Environmental Research, and Atmospheric Systems Research (ASR) program. The Pacific Northwest National Laboratory is operated for DOE by Battelle Memorial Institute under contract DE-AC05-76RL01830. WH, BBP, and JLJ were supported by NSF AGS-1822664 and EPA STAR 83587701-0.

REFERENCES

1. Twomey S, Influence of Pollution on Shortwave Albedo of Clouds. J Atmos Sci 1977, 34 (7), 1149–1152.
2. Dockery DW; Pope CA; Xu XP; Spengler JD; Ware JH; Fay ME; Ferris BG; Speizer FE, An Association between Air-Pollution and Mortality in 6 United-States Cities. New Engl J Med 1993, 329 (24), 1753–1759. [PubMed: 8179653]
3. Zhang Q; Jimenez JL; Canagaratna MR; Allan JD; Coe H; Ulbrich I; Alfarra MR; Takami A; Middlebrook AM; Sun YL; Dzepina K; Dunlea E; Docherty K; DeCarlo PF; Salcedo D; Onasch T; Jayne JT; Miyoshi T; Shimono A; Hatakeyama S; Takegawa N; Kondo Y; Schneider J; Drewnick F; Borrmann S; Weimer S; Demerjian K; Williams P; Bower K; Bahreini R; Cottrell L; Griffin RJ; Rautiainen J; Sun JY; Zhang YM; Worsnop DR, Ubiquity and dominance of oxygenated species in organic aerosols in anthropogenically-influenced Northern Hemisphere midlatitudes. Geophys Res Lett 2007, 34 (13).
4. Jimenez JL; Canagaratna MR; Donahue NM; Prevot ASH; Zhang Q; Kroll JH; DeCarlo PF; Allan JD; Coe H; Ng NL; Aiken AC; Docherty KS; Ulbrich IM; Grieshop AP; Robinson AL; Duplissy J; Smith JD; Wilson KR; Lanz VA; Hueglin C; Sun YL; Tian J; Laaksonen A; Raatikainen T; Rautiainen J; Vaattovaara P; Ehn M; Kulmala M; Tomlinson JM; Collins DR; Cubison MJ; Dunlea EJ; Huffman JA; Onasch TB; Alfarra MR; Williams PI; Bower K; Kondo Y; Schneider J; Drewnick F; Borrmann S; Weimer S; Demerjian K; Salcedo D; Cottrell L; Griffin R; Takami A; Miyoshi T; Hatakeyama S; Shimono A; Sun JY; Zhang YM; Dzepina K; Kimmel JR; Sueper D; Jayne JT; Herndon SC; Trimborn AM; Williams LR; Wood EC; Middlebrook AM; Kolb CE; Baltensperger U; Worsnop DR, Evolution of Organic Aerosols in the Atmosphere. Science 2009, 326 (5959), 1525–1529. [PubMed: 20007897]

5. Goldstein AH; Galbally IE, Known and unexplored organic constituents in the earth's atmosphere. Environ Sci Technol 2007, 41 (5), 1514–1521. [PubMed: 17396635]

6. Weber RJ; Sullivan AP; Peltier RE; Russell A; Yan B; Zheng M; de Gouw J; Warneke C; Brock C; Holloway JS; Atlas EL; Edgerton E, A study of secondary organic aerosol formation in the anthropogenic-influenced southeastern United States. J Geophys Res-Atmos 2007, 112 (D13).

7. de Gouw JA; Middlebrook AM; Warneke C; Goldan PD; Kuster WC; Roberts JM; Fehsenfeld FC; Worsnop DR; Canagaratna MR; Pszenny AAP; Keene WC; Marchewka M; Bertman SB; Bates TS, Budget of organic carbon in a polluted atmosphere: Results from the New England Air Quality Study in 2002. J Geophys Res-Atmos 2005, 110 (D16).

8. Pye HOT; D'Ambro EL; Lee B; Schobesberger S; Takeuchi M; Zhao Y; Lopez-Hilfiker F; Liu JM; Shilling JE; Xing J; Mathur R; Middlebrook AM; Liao J; Welti A; Graus M; Warneke C; de Gouw JA; Holloway JS; Ryerson TB; Pollack IB; Thornton JA, Anthropogenic enhancements to production of highly oxygenated molecules from autoxidation. P Natl Acad Sci USA 2019, 116 (14), 6641–6646.

9. Shilling JE; Zaveri RA; Fast JD; Kleinman L; Alexander ML; Canagaratna MR; Fortner E; Hubbe JM; Jayne JT; Sedlacek A; Setyan A; Springston S; Worsnop DR; Zhang Q, Enhanced SOA formation from mixed anthropogenic and biogenic emissions during the CARES campaign. Atmos Chem Phys 2013, 13 (4), 2091–2113.

10. Shrivastava M; Andreae MO; Artaxo P; Barbosa HMJ; Berg LK; Brito J; Ching J; Easter RC; Fan JW; Fast JD; Feng Z; Fuentes JD; Glasius M; Goldstein AH; Alves EG; Gomes H; Gu D; Guenther A; Jathar SH; Kim S; Liu Y; Lou SJ; Martin ST; McNeill VF; Medeiros A; de Sa SS; Shilling JE; Springston SR; Souza RAF; Thornton JA; Isaacman-VanWertz G; Yee LD; Ynoue R; Zaveri RA; Zelenyuk A; Zhao C, Urban pollution greatly enhances formation of natural aerosols over the Amazon rainforest. Nat Commun 2019, 10.

11. Miller MS; Hidy GM; Friedlander SK, Chemical Element Balance for Pasadena Aerosol. J Colloid Interf Sci 1972, 39 (1), 165–+.

12. Lopez-Hilfiker FD; Mohr C; Ehn M; Rubach F; Kleist E; Wildt J; Mentel TF; Lutz A; Hallquist M; Worsnop D; Thornton JA, A novel method for online analysis of gas and particle composition: description and evaluation of a Filter Inlet for Gases and AEROsols (FIGAERO). Atmos Meas Tech 2014, 7 (4), 983–1001.

13. Lopez-Hilfiker FD; Pospisilova V; Huang W; Kalberer M; Mohr C; Stefenelli G; Thornton JA; Baltensperger U; Prevot ASH; Slowik JG, An extractive electrospray ionization time-of-flight mass spectrometer (EESI-TOF) for online measurement of atmospheric aerosol particles. Atmos. Meas. Tech 2019, 12 (9), 4867–4886.

14. Williams BJ; Goldstein AH; Kreisberg NM; Hering SV, An in-situ instrument for speciated organic composition of atmospheric aerosols: Thermal Desorption Aerosol GC/MS-FID (TAG). Aerosol Sci Tech 2006, 40 (8), 627–638.

15. Zuth C; Vogel AL; Ockenfeld S; Huesmann R; Hoffmann T, Ultrahigh-Resolution Mass Spectrometry in Real Time: Atmospheric Pressure Chemical Ionization Orbitrap Mass Spectrometry of Atmospheric Organic Aerosol. Anal Chem 2018, 90 (15), 8816–8823. [PubMed: 29961316]

16. Carlton AG; de Gouw J; Jimenez JL; Ambrose JL; Attwood AR; Brown S; Baker KR; Brock C; Cohen RC; Edgerton S; Farkas CM; Farmer D; Goldstein AH; Gratz L; Guenther A; Hunt S; Jaegle L; Jaffe DA; Mak J; McClure C; Nenes A; Nguyen TK; Pierce JR; de Sa S; Selin NE; Shah V; Shaw S; Shepson PB; Song SJ; Stutz J; Surratt JD; Turpin BJ; Warneke C; Washenfelder RA; Wennberg PO; Zhou XL, SYNTHESIS OF THE SOUTHEAST ATMOSPHERE STUDIES: Investigating Fundamental Atmospheric Chemistry Questions. B Am Meteorol Soc 2018, 99 (3), 547–567.

17. Petaja T; O'Connor EJ; Moisseev D; Sinclair VA; Manninen AJ; Vaananen R; von Lerber A; Thorntoton JA; Nicocoll K; Petersen W; Chandrasekar V; Smith JN; Winkler PM; Kruger O; Hakola H; Timonen H; Brus D; Laurila T; Asmi E; Riekkola ML; Mona L; Massoli P; Engelmann R; Kompppula M; Wang J; Kuang CG; Back J; Virtanen A; Levula J; Ritsche M; Hickmon N, Baecc a Field Campaign to Elucidate the Impact of Biogenic Aerosols on Clouds and Climate. B Am Meteorol Soc 2016, 97 (10), 1909–1928.

18. Jayne JT; Leard DC; Zhang XF; Davidovits P; Smith KA; Kolb CE; Worsnop DR, Development of an aerosol mass spectrometer for size and composition analysis of submicron particles. Aerosol Sci Tech 2000, 33 (1–2), 49–70.

19. Lee BH; Lopez-Hilfiker FD; Mohr C; Kurten T; Worsnop DR; Thornton JA, An Iodide-Adduct High-Resolution Time-of-Flight Chemical-Ionization Mass Spectrometer: Application to Atmospheric Inorganic and Organic Compounds. Environ Sci Technol 2014, 48 (11), 6309–6317. [PubMed: 24800638]

20. Liu S; Shilling JE; Song C; Hiranuma N; Zaveri RA; Russell LM, Hydrolysis of Organonitrate Functional Groups in Aerosol Particles. Aerosol Sci Tech 2012, 46 (12), 1359–1369.

21. Simoneit BRT; Schauer JJ; Nolte CG; Oros DR; Elias VO; Fraser MP; Rogge WF; Cass GR, Levoglucosan, a tracer for cellulose in biomass burning and atmospheric particles. Atmos Environ 1999, 33 (2), 173–182.

22. Murphy BN; Woody MC; Jimenez JL; Carlton AMG; Hayes PL; Liu S; Ng NL; Russell LM; Setyan A; Xu L; Young J; Zaveri RA; Zhang Q; Pye HOT, Semivolatile POA and parameterized total combustion SOA in CMAQv5.2: impacts on source strength and partitioning. Atmos Chem Phys 2017, 17 (18), 11107–11133. [PubMed: 32038726]

23. Xu L; Pye HOT; He J; Chen YL; Murphy BN; Ng NL, Experimental and model estimates of the contributions from biogenic monoterpenes and sesquiterpenes to secondary organic aerosol in the southeastern United States. Atmos Chem Phys 2018, 18 (17), 12613–12637. [PubMed: 30853976]

24. Pye HOT; Luecken DJ; Xu L; Boyd CM; Ng NL; Baker KR; Ayres BR; Bash JO; Baumann K; Carter WPL; Edgerton E; Fry JL; Hutzell WT; Schwede DB; Shepson PB, Modeling the Current and Future Roles of Particulate Organic Nitrates in the Southeastern United States. Environ Sci Technol 2015, 49 (24), 14195–14203. [PubMed: 26544021]

25. Pye HOT; Pinder RW; Piletic IR; Xie Y; Capps SL; Lin YH; Surratt JD; Zhang ZF; Gold A; Luecken DJ; Hutzell WT; Jaoui M; Offenberg JH; Kleindienst TE; Lewandowski M; Edney EO, Epoxide Pathways Improve Model Predictions of Isoprene Markers and Reveal Key Role of Acidity in Aerosol Formation. Environ Sci Technol 2013, 47 (19), 11056–11064. [PubMed: 24024583]

26. Carlton AG; Bhave PV; Napelenok SL; Edney ED; Sarwar G; Pinder RW; Pouliot GA; Houyoux M, Model Representation of Secondary Organic Aerosol in CMAQv4.7. Environ Sci Technol 2010, 44 (22), 8553–8560. [PubMed: 20883028]

27. Pye HOT; Murphy BN; Xu L; Ng NL; Carlton AG; Guo HY; Weber R; Vasilakos P; Appel KW; Budisulistiorini SH; Surratt JD; Nenes A; Hu WW; Jimenez JL; Isaacman-VanWertz G; Misztal PK; Goldstein AH, On the implications of aerosol liquid water and phase separation for organic aerosol mass. Atmos Chem Phys 2017, 17 (1), 343–369. [PubMed: 30147709]

28. Carlton AG; Turpin BJ; Altieri KE; Seitzinger SP; Mathur R; Roselle SJ; Weber RJ, CMAQ Model Performance Enhanced When In-Cloud Secondary Organic Aerosol is Included: Comparisons of Organic Carbon Predictions with Measurements. Environ Sci Technol 2008, 42 (23), 8798–8802. [PubMed: 19192800]

29. Kenseth CM; Huang YL; Zhao R; Dalleska NF; Hethcox C; Stoltz BM; Seinfeld JH, Synergistic O-3 + OH oxidation pathway to extremely low-volatility dimers revealed in beta-pinene secondary organic aerosol. P Natl Acad Sci USA 2018, 115 (33), 8301–8306.

30. Zhang HF; Yee LD; Lee BH; Curtis MP; Worton DR; Isaacman-VanWertz G; Offenberg JH; Lewandowski M; Kleindienst TE; Beaver MR; Holder AL; Lonneman WA; Docherty KS; Jaoui M; Pye HOT; Hu WW; Day DA; Campuzano-Jost P; Jimenez JL; Guo HY; Weber RJ; de Gouw J; Koss AR; Edgerton ES; Brune W; Mohr C; Lopez-Hilfiker FD; Lutz A; Kreisberg NM; Spielman SR; Hering SV; Wilson KR; Thornton JA; Goldstein AH, Monoterpenes are the largest source of summertime organic aerosol in the southeastern United States. P Natl Acad Sci USA 2018, 115 (9), 2038–2043.

31. Budisulistiorini SH; Li X; Bairai ST; Renfro J; Liu Y; Liu YJ; McKinney KA; Martin ST; McNeill VF; Pye HOT; Nenes A; Neff ME; Stone EA; Mueller S; Knote C; Shaw SL; Zhang Z; Gold A; Surratt JD, Examining the effects of anthropogenic emissions on isoprene-derived secondary organic aerosol formation during the 2013 Southern Oxidant and Aerosol Study (SOAS) at the Look Rock, Tennessee ground site. Atmos Chem Phys 2015, 15 (15), 8871–8888.

32. Hu WW; Campuzano-Jost P; Palm BB; Day DA; Ortega AM; Hayes PL; Krechmer JE; Chen Q; Kuwata M; Liu YJ; de Sa SS; McKinney K; Martin ST; Hu M; Budisulistiorini SH; Riva M; Surratt JD; St Clair JM; Isaacman-Van Wertz G; Yee LD; Goldstein AH; Carbone S; Brito J; Artaxo P; de Gouw JA; Koss A; Wisthaler A; Mikoviny T; Karl T; Kaser L; Jud W; Hansel A; Docherty KS; Alexander ML; Robinson NH; Coe H; Allan JD; Canagaratna MR; Paulot F; Jimenez JL, Characterization of a real-time tracer for isoprene epoxydiols-derived secondary organic aerosol (IEPOX-SOA) from aerosol mass spectrometer measurements. Atmos Chem Phys 2015, 15 (20), 11807–11833.
33. Hu WW; Palm BB; Day DA; Campuzano-Jost P; Krechmer JE; Peng Z; de Sa SS; Martin ST; Alexander ML; Baumann K; Hacker L; Kiendler-Scharr A; Koss AR; de Gouw JA; Goldstein AH; Seco R; Sjostedt SJ; Park JH; Guenther AB; Kim S; Canonaco F; Prevot ASH; Brune WH; Jimenez JL, Volatility and lifetime against OH heterogeneous reaction of ambient isoprene-epoxydiols-derived secondary organic aerosol (IEPOX-SOA). Atmos Chem Phys 2016, 16 (18), 11563–11580.
34. Lopez-Hilfiker FD; Mohr C; D'Ambro EL; Lutz A; Riedel TP; Gaston CJ; Iyer S; Zhang Z; Gold A; Surratt JD; Lee BH; Kurten T; Hu WW; Jimenez J; Hallquist M; Thornton JA, Molecular Composition and Volatility of Organic Aerosol in the Southeastern US: Implications for IEPDX Derived SOA. Environ Sci Technol 2016, 50 (5), 2200–2209. [PubMed: 26811969]
35. Krechmer JE; Day DA; Ziemann PJ; Jimenez JL, Direct Measurements of Gas/Particle Partitioning and Mass Accommodation Coefficients in Environmental Chambers. Environ Sci Technol 2017, 51 (20), 11867–11875. [PubMed: 28858497]
36. Marais EA; Jacob DJ; Jimenez JL; Campuzano-Jost P; Day DA; Hu W; Krechmer J; Zhu L; Kim PS; Miller CC; Fisher JA; Travis K; Yu K; Hanisco TF; Wolfe GM; Arkinson HL; Pye HOT; Froyd KD; Liao J; McNeill VF, Aqueous-phase mechanism for secondary organic aerosol formation from isoprene: application to the southeast United States and co-benefit of SO2 emission controls. Atmos Chem Phys 2016, 16 (3), 1603–1618.
37. Massoli P; Stark H; Canagaratna MR; Krechmer JE; Xu L; Ng NL; Mauldin RL; Yan C; Kimmel J; Misztal PK; Jimenez JL; Jayne JT; Worsnop DR, Ambient Measurements of Highly Oxidized Gas-Phase Molecules during the Southern Oxidant and Aerosol Study (SOAS) 2013. Acs Earth Space Chem 2018, 2 (7), 653–672.
38. D'Ambro EL; Schobesberger S; Gaston CJ; Lopez-Hilfiker FD; Lee BH; Liu JM; Zelenyuk A; Bell D; Cappa CD; Helgestad T; Li ZY; Guenther A; Wang J; Wise M; Caylor R; Surratt JD; Riedel T; Hyttinen N; Salo VT; Hasan G; Kurten T; Shilling JE; Thornton JA, Chamber-based insights into the factors controlling epoxydiol (IEPOX) secondary organic aerosol (SOA) yield, composition, and volatility. Atmos Chem Phys 2019, 19 (17), 11253–11265.
39. Hu KS; Darer AI; Elrod MJ, Thermodynamics and kinetics of the hydrolysis of atmospherically relevant organonitrates and organosulfates. Atmos Chem Phys 2011, 11 (16), 8307–8320.
40. Jacobs MI; Burke WJ; Elrod MJ, Kinetics of the reactions of isoprene-derived hydroxynitrates: gas phase epoxide formation and solution phase hydrolysis. Atmos Chem Phys 2014, 14 (17), 8933–8946.
41. Lee BH; Mohr C; Lopez-Hilfiker FD; Lutz A; Hallquist M; Lee L; Romer P; Cohen RC; Iyer S; Kurten T; Hu WW; Day DA; Campuzano-Jost P; Jimenez JL; Xu L; Ng NL; Guo HY; Weber RJ; Wild RJ; Brown SS; Koss A; de Gouw J; Olson K; Goldstein AH; Seco R; Kim S; McAvey K; Shepson PB; Starn T; Baumann K; Edgerton ES; Liu JM; Shilling JE; Miller DO; Brune W; Schobesberger S; D'Ambro EL; Thornton JA, Highly functionalized organic nitrates in the southeast United States: Contribution to secondary organic aerosol and reactive nitrogen budgets. P Natl Acad Sci USA 2016, 113 (6), 1516–1521.
42. Rindelaub JD; Borca CH; Hostetler MA; Slade JH; Lipton MA; Slipchenko LV; Shepson PB, The acid-catalyzed hydrolysis of an alpha-pinene-derived organic nitrate: kinetics, products, reaction mechanisms, and atmospheric impact. Atmos Chem Phys 2016, 16 (23), 15425–15432.
43. Zare A; Fahey KM; Sarwar G; Cohen RC; Pye HOT, Vapor-Pressure Pathways Initiate but Hydrolysis Products Dominate the Aerosol Estimated from Organic Nitrates. Acs Earth Space Chem 2019, 3 (8), 1426–1437. [PubMed: 31667449]

44. Takeuchi M; Ng NL, Chemical composition and hydrolysis of organic nitrate aerosol formed from hydroxyl and nitrate radical oxidation of alpha-pinene and beta-pinene. Atmos Chem Phys 2019, 19 (19), 12749–12766.
45. Nah T; Sanchez J; Boyd CM; Ng NL, Photochemical Aging of α-pinene and β-pinene Secondary Organic Aerosol formed from Nitrate Radical Oxidation. Environ Sci Technol 2016, 50 (1), 222–231. [PubMed: 26618657]
46. Donahue NM; Henry KM; Mentel TF; Kiendler-Scharr A; Spindler C; Bohn B; Brauers T; Dorn HP; Fuchs H; Tillmann R; Wahner A; Saathoff H; Naumann KH; Mohler O; Leisner T; Muller L; Reinnig MC; Hoffmann T; Salo K; Hallquist M; Frosch M; Bilde M; Tritscher T; Barmet P; Praplan AP; DeCarlo PF; Dommen J; Prevot ASH; Baltensperger U, Aging of biogenic secondary organic aerosol via gas-phase OH radical reactions. P Natl Acad Sci USA 2012, 109 (34), 13503–13508.
47. D'Ambro EL; Schobesberger S; Zaveri RA; Shilling JE; Lee BH; Lopez-Hilfiker FD; Mohr C; Thornton JA, Isothermal Evaporation of alpha-Pinene Ozonolysis SOA: Volatility, Phase State, and Oligomeric Composition. Acs Earth Space Chem 2018, 2 (10), 1058–1067.
48. Capouet M; Muller JF, A group contribution method for estimating the vapour pressures of alpha-pinene oxidation products. Atmos Chem Phys 2006, 6, 1455–1467.
49. Atkinson R; Carter WPL; Winer AM, Effects of Temperature and Pressure on Alkyl Nitrate Yields in the Nox Photooxidations of Normal-Pentane and Normal-Heptane. J Phys Chem-Us 1983, 87 (11), 2012–2018.
50. Berndt T; Richters S; Jokinen T; Hyttinen N; Kurten T; Otkjaer RV; Kjaergaard HG; Stratmann F; Herrmann H; Sipila M; Kulmala M; Ehn M, Hydroxyl radical-induced formation of highly oxidized organic compounds. Nat Commun 2016, 7.
51. Xu L; Moller KH; Crounse JD; Otkjwr RV; Kjaergaard HG; Wennberg PO, Unimolecular Reactions of Peroxy Radicals Formed in the Oxidation of alpha-Pinene and beta-Pinene by Hydroxyl Radicals. J Phys Chem A 2019, 123 (8), 1661–1674. [PubMed: 30700088]
52. Zhao Y; Thornton JA; Pye HOT, Quantitative constraints on autoxidation and dimer formation from direct probing of monoterpene-derived peroxy radical chemistry. P Natl Acad Sci USA 2018, 115 (48), 12142–12147.
53. Ehn M; Thornton JA; Kleist E; Sipila M; Junninen H; Pullinen I; Springer M; Rubach F; Tillmann R; Lee B; Lopez-Hilfiker F; Andres S; Acir IH; Rissanen M; Jokinen T; Schobesberger S; Kangasluoma J; Kontkanen J; Nieminen T; Kurten T; Nielsen LB; Jorgensen S; Kjaergaard HG; Canagaratna M; Dal Maso M; Berndt T; Petaja T; Wahner A; Kerminen VM; Kulmala M; Worsnop DR; Wildt J; Mentel TF, A large source of low-volatility secondary organic aerosol. Nature 2014, 506 (7489), 476–+. [PubMed: 24572423]
54. Ng NL; Chhabra PS; Chan AWH; Surratt JD; Kroll JH; Kwan AJ; McCabe DC; Wennberg PO; Sorooshian A; Murphy SM; Dalleska NF; Flagan RC; Seinfeld JH, Effect of NOx level on secondary organic aerosol (SOA) formation from the photooxidation of terpenes. Atmos Chem Phys 2007, 7 (19), 5159–5174.
55. Sarrafzadeh M; Wildt J; Pullinen I; Springer M; Kleist E; Tillmann R; Schmitt SH; Wu C; Mentel TF; Zhao DF; Hastie DR; Kiendler-Scharr A, Impact of NOx and OH on secondary organic aerosol formation from beta-pinene photooxidation. Atmos Chem Phys 2016, 16 (17), 11237–11248.
56. Molteni U; Bianchi F; Klein F; El Haddad I; Frege C; Rossi MJ; Dommen J; Baltensperger U, Formation of highly oxygenated organic molecules from aromatic compounds. Atmos Chem Phys 2018, 18 (3), 1909–1921.
57. Ervens B; Turpin BJ; Weber RJ, Secondary organic aerosol formation in cloud droplets and aqueous particles (aqSOA): a review of laboratory, field and model studies. Atmos Chem Phys 2011, 11 (21), 11069–11102.
58. Qi L; Nakao S; Tang P; Cocker DR, Temperature effect on physical and chemical properties of secondary organic aerosol from m-xylene photooxidation. Atmos Chem Phys 2010, 10 (8), 3847–3854.
59. Ding X; Zheng M; Edgerton ES; Jansen JJ; Wang XM, Contemporary or Fossil Origin: Split of Estimated Secondary Organic Carbon in the Southeastern United States. Environ Sci Technol 2008, 42 (24), 9122–9128. [PubMed: 19174881]

60. Kim PS; Jacob DJ; Fisher JA; Travis K; Yu K; Zhu L; Yantosca RM; Sulprizio MP; Jimenez JL; Campuzano-Jost P; Froyd KD; Liao J; Hair JW; Fenn MA; Butler CF; Wagner NL; Gordon TD; Welti A; Wennberg PO; Crounse JD; St Clair JM; Teng AP; Millet DB; Schwarz JP; Markovic MZ; Perring AE, Sources, seasonality, and trends of southeast US aerosol: an integrated analysis of surface, aircraft, and satellite observations with the GEOS-Chem chemical transport model. Atmos Chem Phys 2015, 15 (18), 10411–10433.

61. Henry KM; Donahue NM, Photochemical Aging of alpha-Pinene Secondary Organic Aerosol: Effects of OH Radical Sources and Photolysis. J Phys Chem A 2012, 116 (24), 5932–5940. [PubMed: 22439909]

62. O'Brien RE; Kroll JH, Photolytic Aging of Secondary Organic Aerosol: Evidence for a Substantial Photo-Recalcitrant Fraction. J Phys Chem Lett 2019, 10 (14), 4003–4009. [PubMed: 31264874]

63. Wong JPS; Zhou SM; Abbatt JPD, Changes in Secondary Organic Aerosol Composition and Mass due to Photolysis: Relative Humidity Dependence. J Phys Chem A 2015, 119 (19), 4309–4316. [PubMed: 25196234]

64. Vaden TD; Imre D; Beranek J; Shrivastava M; Zelenyuk A, Evaporation kinetics and phase of laboratory and ambient secondary organic aerosol. P Natl Acad Sci USA 2011, 108 (6), 2190–2195.

65. Kurten T; Rissanen MP; Mackeprang K; Thornton JA; Hyttinen N; Jorgensen S; Ehn M; Kjaergaard HG, Computational Study of Hydrogen Shifts and Ring-Opening Mechanisms in alpha-Pinene Ozonolysis Products. J Phys Chem A 2015, 119 (46), 11366–11375. [PubMed: 26529548]

66. Claflin MS; Krechmer JE; Hu WW; Jimenez JL; Ziemann PJ, Functional Group Composition of Secondary Organic Aerosol Formed from Ozonolysis of alpha-Pinene Under High VOC and Autoxidation Conditions. Acs Earth Space Chem 2018, 2 (11), 1196–1210.

67. Krapf M; El Haddad I; Bruns EA; Molteni U; Daellenbach KR; Prevot ASH; Baltensperger U; Dommen J, Labile Peroxides in Secondary Organic Aerosol. Chem-Us 2016, 1 (4), 603–616.

68. Shiraiwa M; Yee LD; Schilling KA; Loza CL; Craven JS; Zuend A; Ziemann PJ; Seinfeld JH, Size distribution dynamics reveal particle-phase chemistry in organic aerosol formation. P Natl Acad Sci USA 2013, 110 (29), 11746–11750.

69. McFiggans G; Mentel TF; Wildt J; Pullinen I; Kang S; Kleist E; Schmitt S; Springer M; Tillmann R; Wu C; Zhao DF; Hallquist M; Faxon C; Le Breton M; Hallquist AM; Simpson D; Bergstrom R; Jenkin ME; Ehn M; Thornton JA; Alfarra MR; Bannan TJ; Percival CJ; Priestley M; Topping D; Kiendler-Scharr A, Secondary organic aerosol reduced by mixture of atmospheric vapours. Nature 2019, 565 (7741), 587–593. [PubMed: 30700872]

70. Shilling JE; Zawadowicz MA; Liu JM; Zaveri RA; Zelenyuk A, Photochemical Aging Alters Secondary Organic Aerosol Partitioning Behavior. Acs Earth Space Chem 2019, 3 (22), 2704–2716.

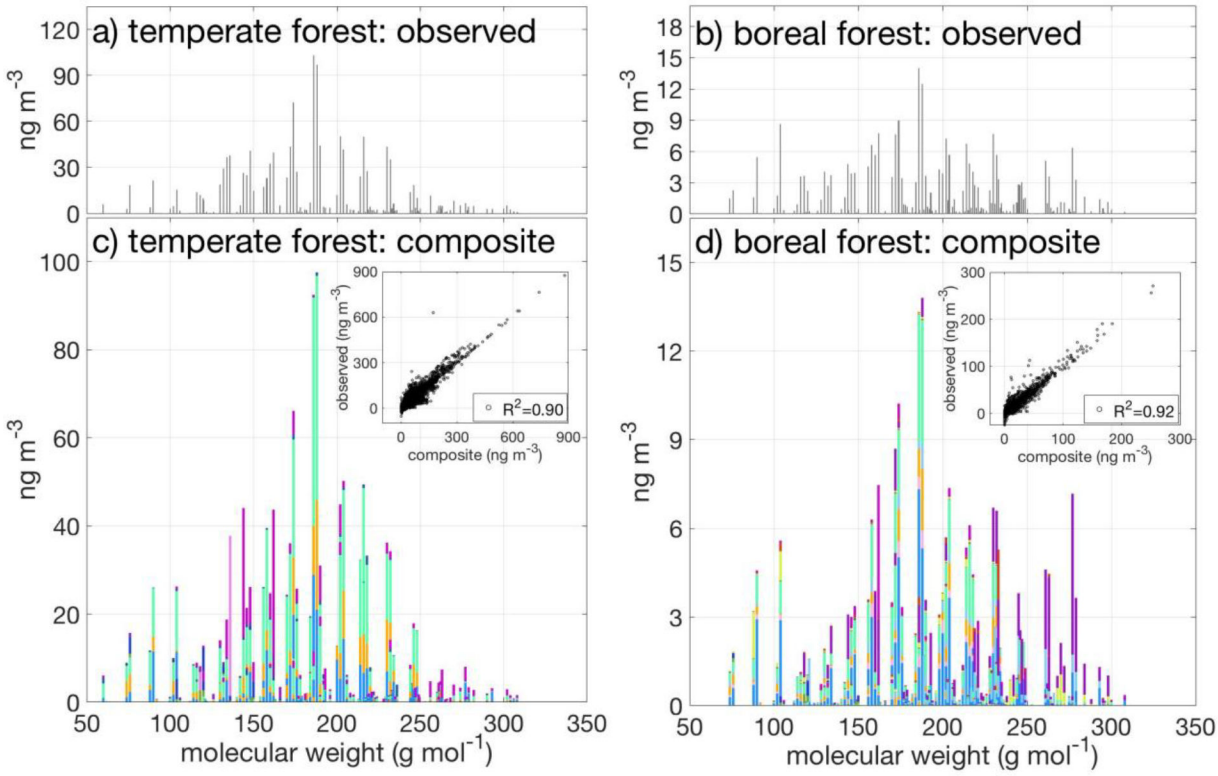

Figure 1.

Median mass distribution of OA components observed during (a) SOAS and (b) BAECC using the FIGAERO-CIMS. Corresponding (c and d) composite spectra generated from the apportionment technique using our basis set. The insets in (c) and (d) show the comparisons between composite and field-observed mass of each organic component ($C_xH_yO_zN_{0–1}$) for all of the ~hourly particle-phase measurements during SOAS and BAECC, respectively, with the correlations in the legends.

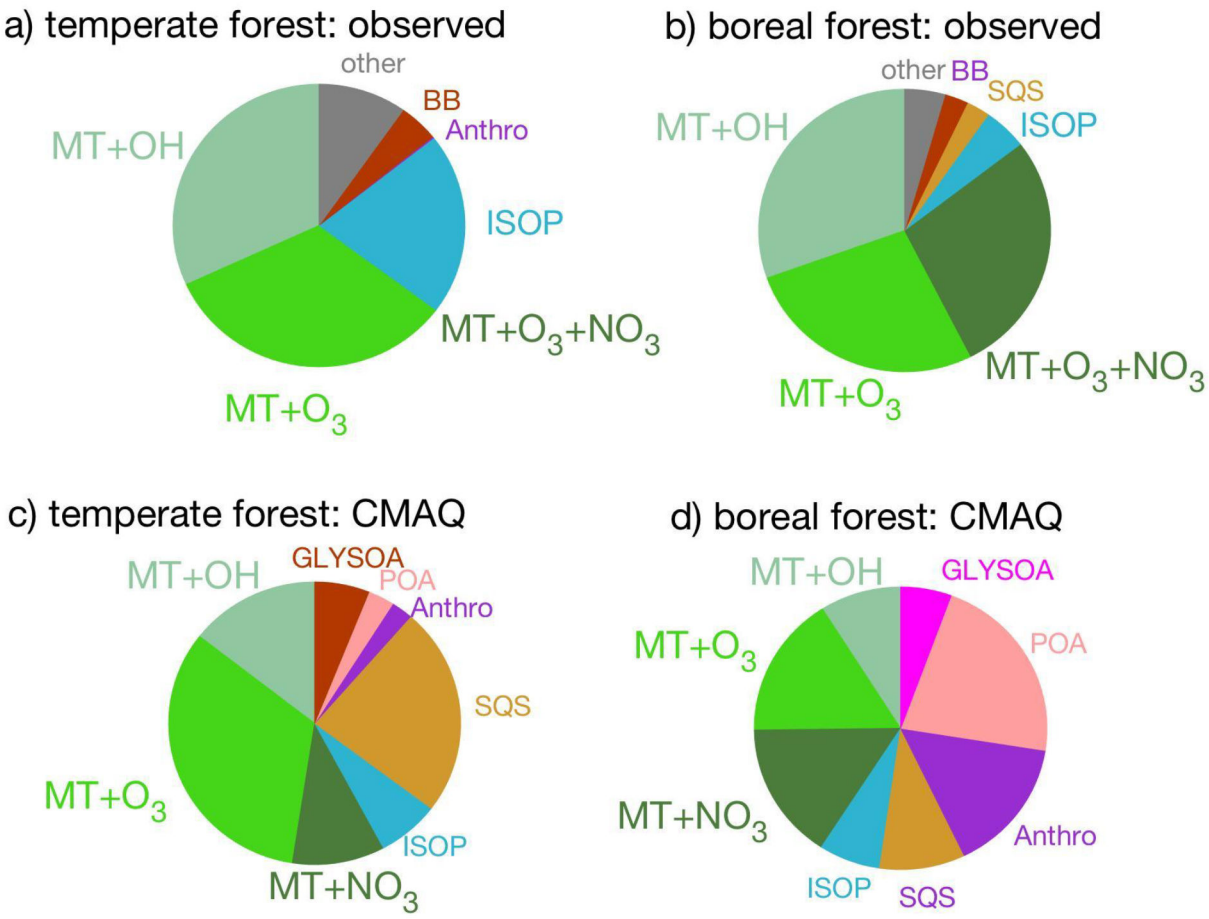

Figure 2.

OA attribution during (a) the SOAS campaign in the temperate mixed forest of the SEUS and (b) during BAECC in the boreal forest of Finland, determined using the FIGAERO-CIMS measurements in the laboratory and ambient atmosphere. Corresponding attribution of OA representing the two sites using CMAQ v5.3 are shown in (c) and (d).

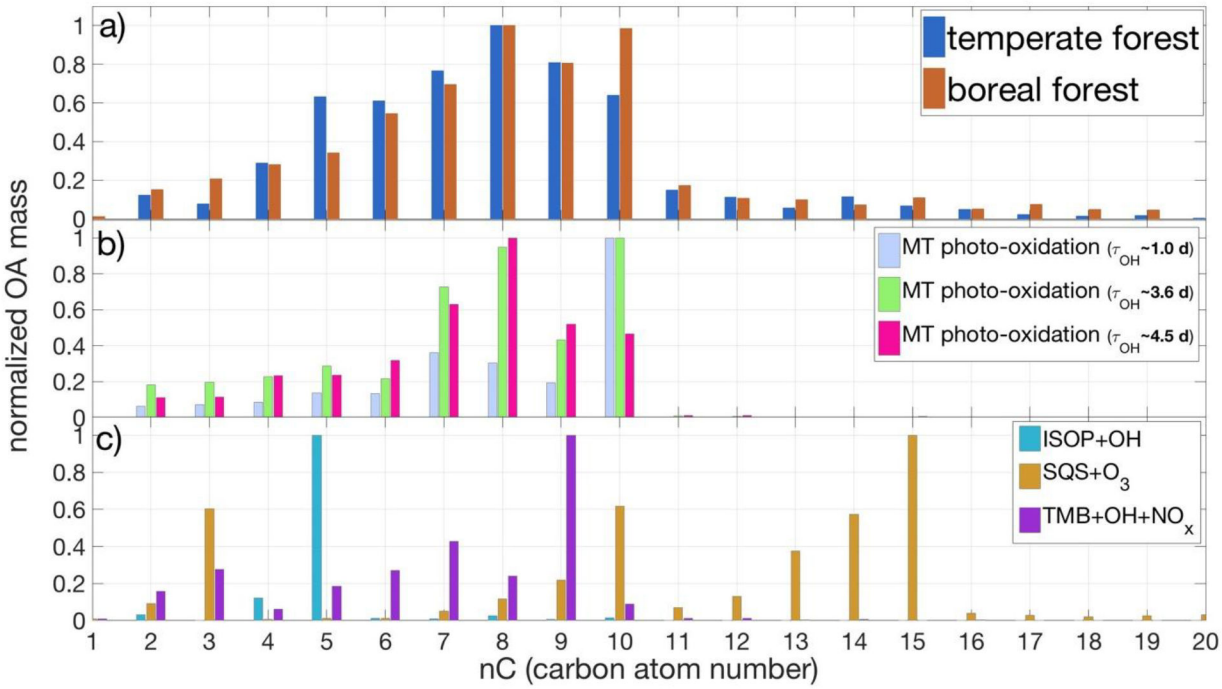

Figure 3.

OA mass distribution as a function of carbon atom number group for (a) the median ambient measurements made in the temperate mixed forest of the SEUS and the boreal forest of Finland, (b) three out of the 10 α-pinene oxidation experiments with varying timescales of OH-oxidation conducted at the PNNL atmospheric simulation chamber, and (c) chamber oxidation experiments involving isoprene, β-caryophyllene, and trimethylbenzene. OA attribution was conducted as illustrated in Figure 1, but composition comparisons in nC space as shown here provides a simple visualization that monoterpene oxidation contibuted significantly to OA mass compared to the oxidation of isoprene, sesquiterpenes, and an anthropogenic proxy as represented by TMB.

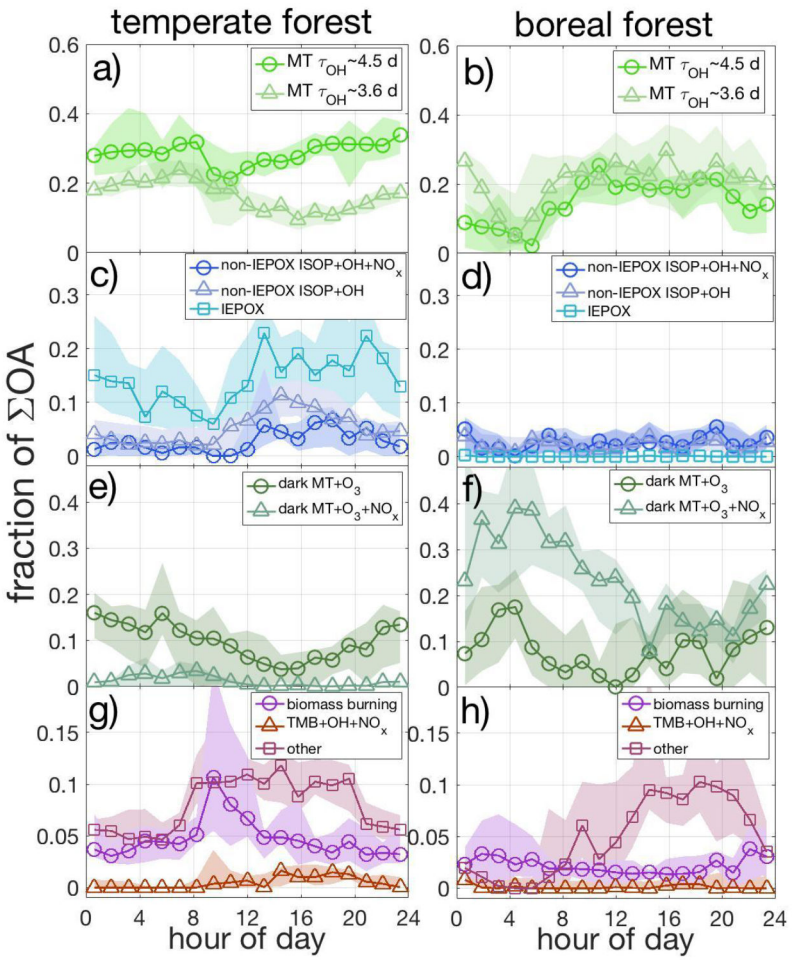

Figure 4.

Fraction of the total OA mass attributed to the most prominent VOC precursor and experimental condition pairings, plotted as a function of hour of day for (a, c, e, g) the temperate forest of SOAS and (b, d, f, h) the boreal forest of BAECC. Markers represent campaign median, with the shaded areas representing the 25th/75th percentiles.

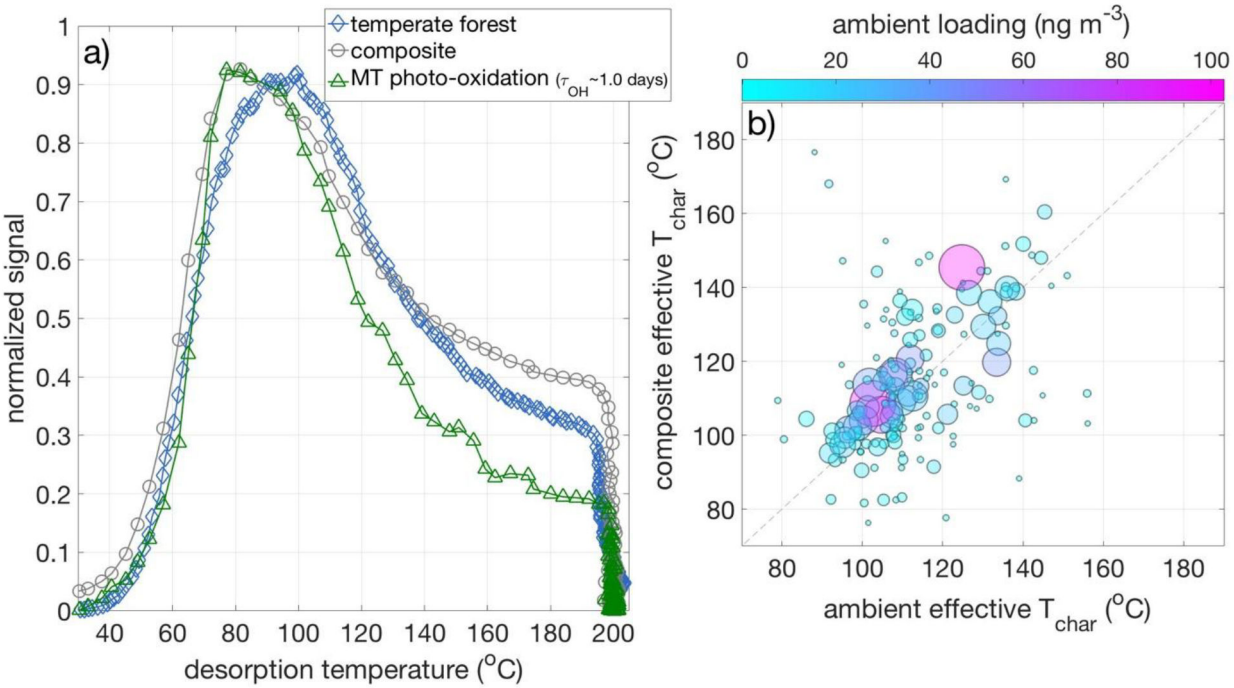

Figure 5.

(a) Median desorption temperature profile of OA observed in a temperate forest during SOAS, along with that of the composite, which was generated as the sum of desorption profiles from all laboratory experiments, each weighted by its contribution to the composite. In comparison, the OA desorption profile observed during an experiment in which α-pinene was oxidized predominantly by OH for only ~1 day exhibited a much higher effective volatility. (b) The median desorption temperature of each of the 175 individual organic compounds observed during SOAS is compared to the effective desorption temperature of the corresponding compounds of the composite. Markers in (b), each representing one of the 175 compounds, is colored by its median abundance in the temperate forest during SOAS and sized by its median abundance of the composite.